

14. QUARK MODEL

Revised October 2007 by C. Amsler (University of Zürich), T. DeGrand (University of Colorado, Boulder) and B. Krusche (University of Basel).

14.1. Quantum numbers of the quarks

Quarks are strongly interacting fermions with spin 1/2 and, by convention, positive parity. Then antiquarks have negative parity. Quarks have the additive baryon number 1/3, antiquarks -1/3. Table 14.1 gives the other additive quantum numbers (flavors) for the three generations of quarks. They are related to the charge Q (in units of the elementary charge e) through the generalized Gell-Mann-Nishijima formula

$$Q = I_z + \frac{\mathcal{B} + S + C + B + T}{2}, \quad (14.1)$$

where \mathcal{B} is the baryon number. The convention is that the *flavor* of a quark (I_z , S , C , B , or T) has the same sign as its *charge* Q . With this convention, any flavor carried by a charged meson has the same sign as its charge, *e.g.*, the strangeness of the K^+ is +1, the bottomness of the B^+ is +1, and the charm and strangeness of the D_s^- are each -1. Antiquarks have the opposite flavor signs.

Table 14.1: Additive quantum numbers of the quarks.

Property \ Quark	d	u	s	c	b	t
Q – electric charge	$-\frac{1}{3}$	$+\frac{2}{3}$	$-\frac{1}{3}$	$+\frac{2}{3}$	$-\frac{1}{3}$	$+\frac{2}{3}$
I – isospin	$\frac{1}{2}$	$\frac{1}{2}$	0	0	0	0
I_z – isospin z -component	$-\frac{1}{2}$	$+\frac{1}{2}$	0	0	0	0
S – strangeness	0	0	-1	0	0	0
C – charm	0	0	0	+1	0	0
B – bottomness	0	0	0	0	-1	0
T – topness	0	0	0	0	0	+1

14.2. Mesons

Mesons have baryon number $\mathcal{B} = 0$. In the quark model, they are $q\bar{q}'$ bound states of quarks q and antiquarks \bar{q}' (the flavors of q and q' may be different). If the orbital angular momentum of the $q\bar{q}'$ state is ℓ , then the parity P is $(-1)^{\ell+1}$. The meson spin J is given by the usual relation $|\ell - s| < J < |\ell + s|$, where s is 0 (antiparallel quark spins) or 1 (parallel quark spins). The charge conjugation, or C -parity $C = (-1)^{\ell+s}$, is defined only for the $q\bar{q}$ states made of quarks and their own antiquarks. The C -parity can be generalized to the G -parity $G = (-1)^{I+\ell+s}$ for mesons made of quarks and their own antiquarks (isospin $I_z = 0$) and for the charged $u\bar{d}$ and $d\bar{u}$ states (isospin $I = 1$).

2 14. Quark model

The mesons are classified in J^{PC} multiplets. The $\ell = 0$ states are the pseudoscalars (0^{-+}) and the vectors (1^{--}). The orbital excitations $\ell = 1$ are the scalars (0^{++}), the axial vectors (1^{++}) and (1^{+-}), and the tensors (2^{++}). Assignments for many of the known mesons are given in Tables 14.2 and 14.3. Radial excitations are denoted by the principal quantum number n . The very short lifetime of the t quark makes it likely that bound state hadrons containing t quarks and/or antiquarks do not exist.

States in the natural spin-parity series $P = (-1)^J$ must, according to the above, have $s = 1$ and hence, $CP = +1$. Thus mesons with natural spin-parity and $CP = -1$ (0^{+-} , 1^{-+} , 2^{+-} , 3^{-+} , etc..) are forbidden in the $q\bar{q}'$ model. The $J^{PC} = 0^{- -}$ state is forbidden as well. Mesons with such *exotic* quantum numbers may exist, but would lie outside the $q\bar{q}'$ model (see section below on exotic mesons).

Following SU(3) the nine possible $q\bar{q}'$ combinations containing the light u , d , and s quarks are grouped into an octet and a singlet of light quark mesons:

$$\mathbf{3} \otimes \bar{\mathbf{3}} = \mathbf{8} \oplus \mathbf{1} . \quad (14.2)$$

A fourth quark such as charm c can be included by extending SU(3) to SU(4). However, SU(4) is badly broken owing to the much heavier c quark. Nevertheless, in an SU(4) classification the sixteen mesons are grouped into a 15-plet and a singlet:

$$\mathbf{4} \otimes \bar{\mathbf{4}} = \mathbf{15} \oplus \mathbf{1} . \quad (14.3)$$

The *weight diagrams* for the ground-state pseudoscalar (0^{-+}) and vector (1^{--}) mesons are depicted in Fig. 14.1. The light quark mesons are members of nonets building the middle plane in Fig. 14.1(a) and (b).

Isoscalar states with the same J^{PC} will mix, but mixing between the two light quark isoscalar mesons, and the much heavier charmonium or bottomonium states, are generally assumed to be negligible. In the following, we shall use the generic names a for the $I = 1$, K for the $I = 1/2$, f and f' for the $I = 0$ members of the light quark nonets. Thus the physical isoscalars are mixtures of the SU(3) wave function ψ_8 and ψ_1 :

$$f' = \psi_8 \cos \theta - \psi_1 \sin \theta , \quad (14.4)$$

$$f = \psi_8 \sin \theta + \psi_1 \cos \theta , \quad (14.5)$$

where θ is the nonet mixing angle and

$$\psi_8 = \frac{1}{\sqrt{6}}(u\bar{u} + d\bar{d} - 2s\bar{s}) , \quad (14.6)$$

$$\psi_1 = \frac{1}{\sqrt{3}}(u\bar{u} + d\bar{d} + s\bar{s}) . \quad (14.7)$$

The mixing angle has to be determined experimentally.

These mixing relations are often rewritten to exhibit the $u\bar{u} + d\bar{d}$ and $s\bar{s}$ components which decouple for the ‘‘ideal’’ mixing angle θ_i such that $\tan \theta_i = 1/\sqrt{2}$ (or $\theta_i = 35.3^\circ$). Defining $\alpha = \theta + 54.7^\circ$, one obtains the physical isoscalar in the flavor basis

$$f' = \frac{1}{\sqrt{2}}(u\bar{u} + d\bar{d}) \cos \alpha - s\bar{s} \sin \alpha , \quad (14.8)$$

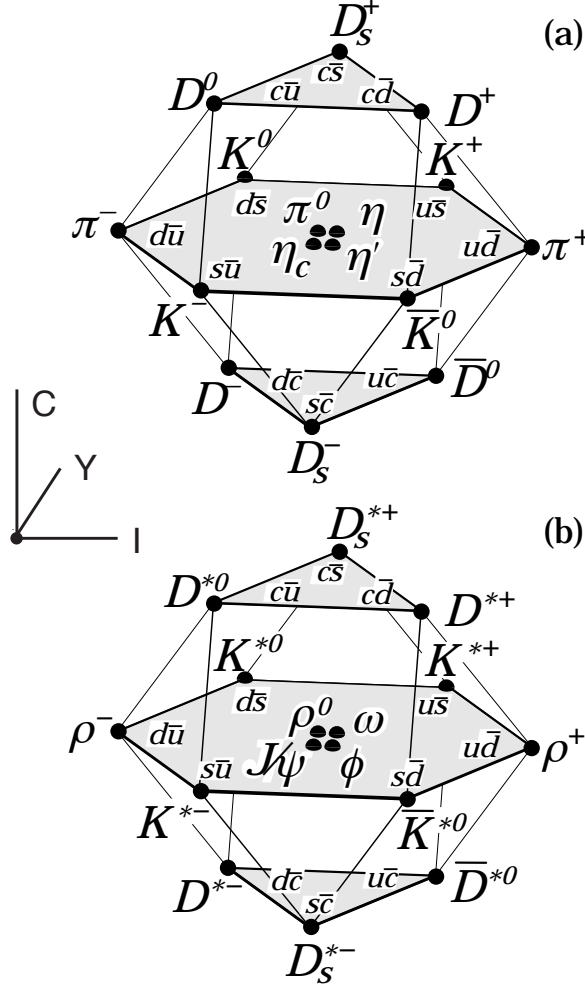


Figure 14.1: SU(4) weight diagram showing the 16-plets for the pseudoscalar (a) and vector mesons (b) made of the u , d , s and c quarks as a function of isospin I , charm C and hypercharge $Y = S+B - \frac{C}{3}$. The nonets of light mesons occupy the central planes to which the $c\bar{c}$ states have been added.

and its orthogonal partner f (replace α by $\alpha - 90^\circ$). Thus for ideal mixing, ($\alpha_i = 90^\circ$) the f' becomes pure $s\bar{s}$ and the f pure $u\bar{u} + d\bar{d}$. The mixing angle θ can be derived from the mass relation

$$\tan \theta = \frac{4m_K - m_a - 3m_{f'}}{2\sqrt{2}(m_a - m_K)}, \quad (14.9)$$

which also determines its sign or, alternatively, from

$$\tan^2 \theta = \frac{4m_K - m_a - 3m_{f'}}{-4m_K + m_a + 3m_f}. \quad (14.10)$$

Eliminating θ from these equations leads to the sum rule [1]

$$(m_f + m_{f'})(4m_K - m_a) - 3m_f m_{f'} = 8m_K^2 - 8m_K m_a + 3m_a^2. \quad (14.11)$$

This relation is verified for the ground-state vector mesons. We identify the $\phi(1020)$ with the f' and the $\omega(783)$ with the f . Thus

$$\phi(1020) = \psi_8 \cos \theta_V - \psi_1 \sin \theta_V, \quad (14.12)$$

4 14. Quark model

$$\omega(782) = \psi_8 \sin \theta_V + \psi_1 \cos \theta_V , \quad (14.13)$$

with the vector mixing angle $\theta_V = 35^\circ$ from Eq. (14.9), very close to ideal mixing. Thus $\phi(1020)$ is nearly pure $s\bar{s}$. For ideal mixing Eq. (14.9) and Eq. (14.10) lead to the relations

$$m_K = \frac{m_f + m_{f'}}{2} , \quad m_a = m_f , \quad (14.14)$$

which are satisfied for the vector mesons. However, for the pseudoscalar (and scalar mesons) Eq. (14.11) is satisfied only approximately. Then Eq. (14.9) and Eq. (14.10) lead to somewhat different values for the mixing angle. Identifying the η with the f' one gets

$$\eta = \psi_8 \cos \theta_P - \psi_1 \sin \theta_P , \quad (14.15)$$

$$\eta' = \psi_8 \sin \theta_P + \psi_1 \cos \theta_P . \quad (14.16)$$

Following chiral perturbation theory, the meson masses in the mass formulae (Eq. (14.9) and Eq. (14.10)) should be replaced by their squares. Table 14.2 lists the mixing angle θ_{lin} from Eq. (14.10) and the corresponding θ_{quad} obtained by replacing the meson masses by their squares throughout.

The pseudoscalar mixing angle θ_P can also be measured by comparing the partial widths for radiative J/ψ decay into a vector and a pseudoscalar [2], radiative $\phi(1020)$ decay into η and η' [3], or $\bar{p}p$ annihilation at rest into a pair of vector and pseudoscalar or into two pseudoscalars [4,5]. One obtains a mixing angle between -10° and -20° .

The nonet mixing angles can be measured in $\gamma\gamma$ collisions, *e.g.* for the 0^{-+} , 0^{++} and 2^{++} nonets. In the quark model the amplitude for the coupling of neutral mesons to two photons is proportional to $\sum_i Q_i^2$, where Q_i is the charge of the i -th quark. The 2γ partial width of an isoscalar meson with mass m is then given in terms of the mixing angle α by

$$\Gamma_{2\gamma} = C(5 \cos \alpha - \sqrt{2} \sin \alpha)^2 m^3 , \quad (14.17)$$

for f' and f ($\alpha \rightarrow \alpha - 90^\circ$). The coupling C may depend on the meson mass. It is often assumed to be a constant in the nonet. For the isovector a , one then finds $\Gamma_{2\gamma} = 9 C m^3$. Thus the members of an ideally mixed nonet couple to 2γ with partial widths in the ratios $f : f' : a = 25 : 2 : 9$. For tensor mesons, one finds from the ratios of the measured 2γ partial widths for the $f_2(1270)$ and $f_2'(1525)$ mesons a mixing angle α_T of $(81 \pm 1)^\circ$, or $\theta_T = (27 \pm 1)^\circ$, in accord with the linear mass formula. For the pseudoscalars, one finds from the ratios of partial widths $\Gamma(\eta' \rightarrow 2\gamma)/\Gamma(\eta \rightarrow 2\gamma)$ a mixing angle $\theta_P = (-18 \pm 2)^\circ$, while the ratio $\Gamma(\eta' \rightarrow 2\gamma)/\Gamma(\pi^0 \rightarrow 2\gamma)$ leads to $\sim -24^\circ$. SU(3) breaking effects for pseudoscalars are discussed in Ref. 6.

Table 14.2: Suggested $q\bar{q}$ quark-model assignments for some of the observed light mesons. Mesons in bold face are included in the Meson Summary Table. The wave functions f and f' are given in the text. The singlet-octet mixing angles from the quadratic and linear mass formulae are also given for the well established nonets. The classification of the 0^{++} mesons is tentative and the mixing angle uncertain due to large uncertainties in some of the masses. Also, the $f_0(1710)$ and $f_0(1370)$ are expected to mix with the $f_0(1500)$. The latter is not in this table as it is hard to accommodate in the scalar nonet. The light scalars $a_0(980)$, $f_0(980)$ and $f_0(600)$ are often considered as meson-meson resonances or four-quark states and are therefore not included in the table. See the “Note on Non- $q\bar{q}$ Mesons” at the end of the Meson Listings.

$n \ 2s+1\ell_J$	J^{PC}	$I = 1$ $u\bar{d}, \bar{u}d, \frac{1}{\sqrt{2}}(d\bar{d} - u\bar{u})$	$I = \frac{1}{2}$ $u\bar{s}, \bar{d}\bar{s}; \bar{d}s, -\bar{u}s$	$I = 0$ f'	$I = 0$ f	θ_{quad} [°]	θ_{lin} [°]
$1 \ ^1S_0$	0^{-+}	π	K	η	$\eta'(958)$	-11.5	-24.6
$1 \ ^3S_1$	1^{--}	$\rho(770)$	$K^*(892)$	$\phi(1020)$	$\omega(782)$	38.7	36.0
$1 \ ^1P_1$	1^{+-}	$b_1(1235)$	K_{1B}^\dagger	$h_1(1380)$	$h_1(1170)$		
$1 \ ^3P_0$	0^{++}	$a_0(1450)$	$K_0^*(1430)$	$f_0(1710)$	$f_0(1370)$		
$1 \ ^3P_1$	1^{++}	$a_1(1260)$	K_{1A}^\dagger	$f_1(1420)$	$f_1(1285)$		
$1 \ ^3P_2$	2^{++}	$a_2(1320)$	$K_2^*(1430)$	$f_2'(1525)$	$f_2(1270)$	29.6	28.0
$1 \ ^1D_2$	2^{-+}	$\pi_2(1670)$	$K_2(1770)^\dagger$	$\eta_2(1870)$	$\eta_2(1645)$		
$1 \ ^3D_1$	1^{--}	$\rho(1700)$	$K^*(1680)^\ddagger$		$\omega(1650)$		
$1 \ ^3D_2$	2^{--}		$K_2(1820)^\ddagger$				
$1 \ ^3D_3$	3^{--}	$\rho_3(1690)$	$K_3^*(1780)$	$\phi_3(1850)$	$\omega_3(1670)$	32.0	31.0
$1 \ ^3F_4$	4^{++}	$a_4(2040)$	$K_4^*(2045)$		$f_4(2050)$		
$1 \ ^3G_5$	5^{--}	$\rho_5(2350)$					
$1 \ ^3H_6$	6^{++}	$a_6(2450)$			$f_6(2510)$		
$2 \ ^1S_0$	0^{-+}	$\pi(1300)$	$K(1460)$	$\eta(1475)$	$\eta(1295)$		
$2 \ ^3S_1$	1^{--}	$\rho(1450)$	$K^*(1410)^\ddagger$	$\phi(1680)$	$\omega(1420)$		

[†] The $1^{+\pm}$ and $2^{-\pm}$ isospin $\frac{1}{2}$ states mix. In particular, the K_{1A} and K_{1B} are nearly equal (45°) mixtures of the $K_1(1270)$ and $K_1(1400)$.

[‡] The $K^*(1410)$ could be replaced by the $K^*(1680)$ as the $2 \ ^3S_1$ state.

6 14. Quark model

Table 14.3: $q\bar{q}$ quark-model assignments for the observed heavy mesons. Mesons in bold face are included in the Meson Summary Table.

$n^{2s+1}\ell_J \quad J^{PC}$	$l = 0$ $c\bar{c}$	$l = 0$ $b\bar{b}$	$l = \frac{1}{2}$ $c\bar{u}, c\bar{d}; \bar{c}u, \bar{c}d$	$l = 0$ $c\bar{s}; \bar{c}s$	$l = \frac{1}{2}$ $b\bar{u}, b\bar{d}; \bar{b}u, \bar{b}d$	$l = 0$ $b\bar{s}; \bar{b}s$	$l = 0$ $b\bar{c}; \bar{b}c$
$1^1S_0 \quad 0^{-+}$	$\eta_c(1S)$	$\eta_b(1S)$	D	D_s^\pm	B	B_s^0	B_c^\pm
$1^3S_1 \quad 1^{--}$	$J/\psi(1S)$	$\Upsilon(1S)$	D^*	$D_s^{*\pm}$	B^*	B_s^*	
$1^1P_1 \quad 1^{+-}$	$h_c(1P)$		$D_1(2420)$	$D_{s1}(2536)^\pm$			
$1^3P_0 \quad 0^{++}$	$\chi_{c0}(1P)$	$\chi_{b0}(1P)$		$D_{s0}^*(2317)^{\pm\dagger}$			
$1^3P_1 \quad 1^{++}$	$\chi_{c1}(1P)$	$\chi_{b1}(1P)$		$D_{s1}(2460)^{\pm\dagger}$			
$1^3P_2 \quad 2^{++}$	$\chi_{c2}(1P)$	$\chi_{b2}(1P)$	$D_2^*(2460)$	$D_{s2}(2573)^\pm$			
$1^3D_1 \quad 1^{--}$	$\psi(3770)$						
$2^1S_0 \quad 0^{-+}$	$\eta_c(2S)$						
$2^3S_1 \quad 1^{--}$	$\psi(2S)$	$\Upsilon(2S)$					
$2^3P_{0,1,2} \quad 0^{++}, 1^{++}, 2^{++}$		$\chi_{b0,1,2}(2P)$					

[†] The masses of these states are considerably smaller than most theoretical predictions. They have also been considered as four-quark states (See the “Note on Non- $q\bar{q}$ Mesons” at the end of the Meson Listings). The $D_{s1}(2460)^\pm$ and $D_{s1}(2536)^\pm$ are mixtures of the $1^{+\pm}$ states.

Table 14.4: SU(3) couplings γ^2 for quarkonium decays as a function of nonet mixing angle α , up to a common multiplicative factor C ($\phi \equiv 54.7^\circ + \theta_P$).

Isospin	Decay channel	γ^2
0	$\pi\pi$	$3 \cos^2 \alpha$
	$K\bar{K}$	$(\cos \alpha - \sqrt{2} \sin \alpha)^2$
	$\eta\eta$	$(\cos \alpha \cos^2 \phi - \sqrt{2} \sin \alpha \sin^2 \phi)^2$
	$\eta\eta'$	$\frac{1}{2} \sin^2 2\phi (\cos \alpha + \sqrt{2} \sin \alpha)^2$
1	$\eta\pi$	$2 \cos^2 \phi$
	$\eta'\pi$	$2 \sin^2 \phi$
	$K\bar{K}$	1
$\frac{1}{2}$	$K\pi$	$\frac{3}{2}$
	$K\eta$	$(\sin \phi - \frac{\cos \phi}{\sqrt{2}})^2$
	$K\eta'$	$(\cos \phi + \frac{\sin \phi}{\sqrt{2}})^2$

The partial width for the decay of a scalar or a tensor meson into a pair of pseudoscalar mesons is model dependent. Following Ref. 7,

$$\Gamma = C \times \gamma^2 \times |F(q)|^2 \times q . \quad (14.18)$$

C is a nonet constant, q the momentum of the decay products, $F(q)$ a form factor and γ^2 the SU(3) coupling. The model-dependent form factor may be written as

$$|F(q)|^2 = q^{2\ell} \times \exp(-\frac{q^2}{8\beta^2}), \quad (14.19)$$

where ℓ is the relative angular momentum between the decay products. The decay of a $q\bar{q}$ meson into a pair of mesons involves the creation of a $q\bar{q}$ pair from the vacuum, and SU(3) symmetry assumes that the matrix elements for the creation of $s\bar{s}$, $u\bar{u}$ and $d\bar{d}$ pairs are equal. The couplings γ^2 are given in Table 14.4 and their dependence upon the mixing angle α is shown in Fig. 14.2 for isoscalar decays. The generalization to unequal $s\bar{s}$, $u\bar{u}$, and $d\bar{d}$ couplings is given in Ref. 7. An excellent fit to the tensor meson decay widths is obtained assuming SU(3) symmetry, with $\beta \simeq 0.5$ GeV/c, $\theta_V \simeq 26^\circ$ and $\theta_P \simeq -17^\circ$ [7].

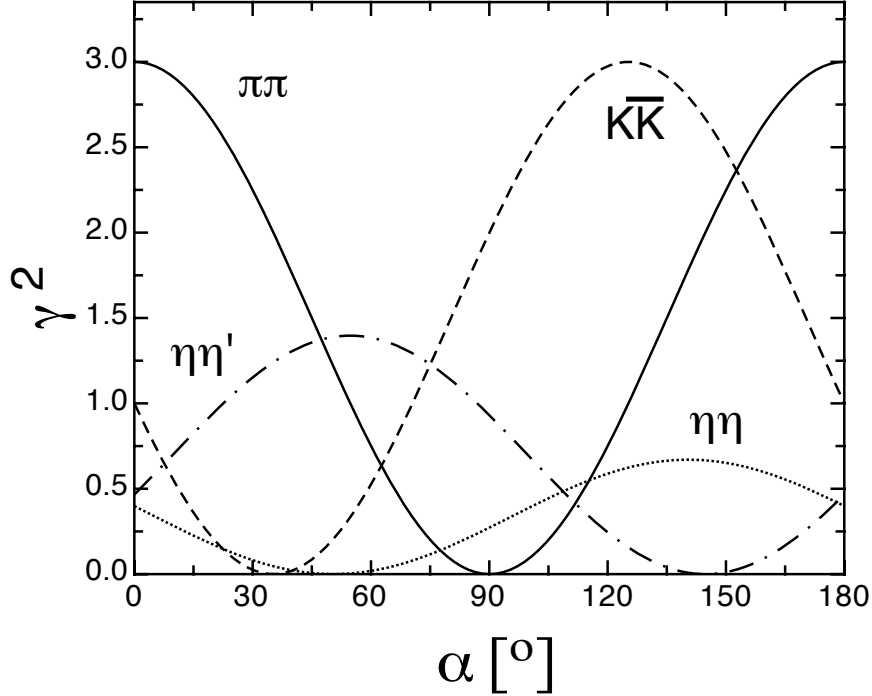


Figure 14.2: SU(3) couplings as a function of mixing angle α for isoscalar decays, up to a common multiplicative factor C and for $\theta_P = -17.3^\circ$ (from Ref. 4).

14.3. Exotic mesons

The existence of a light nonet composed of four quarks with masses below 1 GeV was suggested a long time ago [8]. Coupling two triplets of light quarks u , d , and s , one obtains nine states, of which the six symmetric (uu , dd , ss , $ud + du$, $us + su$, $ds + sd$) form the six dimensional representation $\mathbf{6}$, while the three antisymmetric ($ud - du$, $us - su$, $ds - sd$) form the three dimensional representation $\bar{\mathbf{3}}$ of SU(3):

$$\mathbf{3} \otimes \mathbf{3} = \mathbf{6} \oplus \bar{\mathbf{3}}. \quad (14.20)$$

Combining with spin and color and requiring antisymmetry, one finds that the most deeply bound diquark (and hence the lightest) is the one in the $\bar{\mathbf{3}}$ and spin singlet state. The combination of the diquark with an antidiquark in the $\mathbf{3}$ representation then gives a light nonet of four-quark scalar states. Letting the number of strange quarks determine the mass splitting, one obtains a mass inverted spectrum with a light isosinglet ($ud\bar{u}\bar{d}$), a medium heavy isodoublet (*e.g.*, $ud\bar{s}\bar{d}$) and a heavy isotriplet (*eg*, $ds\bar{u}\bar{s}$) + isosinglet (*e.g.*, $us\bar{u}\bar{s}$). It is then tempting to identify the lightest state with the $f_0(600)$, and the heaviest states with the $a_0(980)$, and $f_0(980)$. Then the meson with strangeness $\kappa(800)$ would lie in between.

QCD predicts the existence of isoscalar mesons which contain only gluons, the glueballs. The ground state glueball is predicted by lattice gauge theories to be 0^{++} , the first excited state 2^{++} . Errors on the mass predictions are large. As an example for the glueball mass spectrum, we show in Figure 14.3 a recent calculation from the lattice [9] (see also [10]). This group predicts a mass of 1710 MeV for the ground state, with an error of about 100 MeV. Earlier work by other groups produced masses at 1650 MeV [11] and 1550 MeV [12] (see also Ref. 13). The first excited state has a mass of about 2.4 GeV and the lightest glueball with exotic quantum numbers (2^{+-}) has a mass of about 4 GeV.

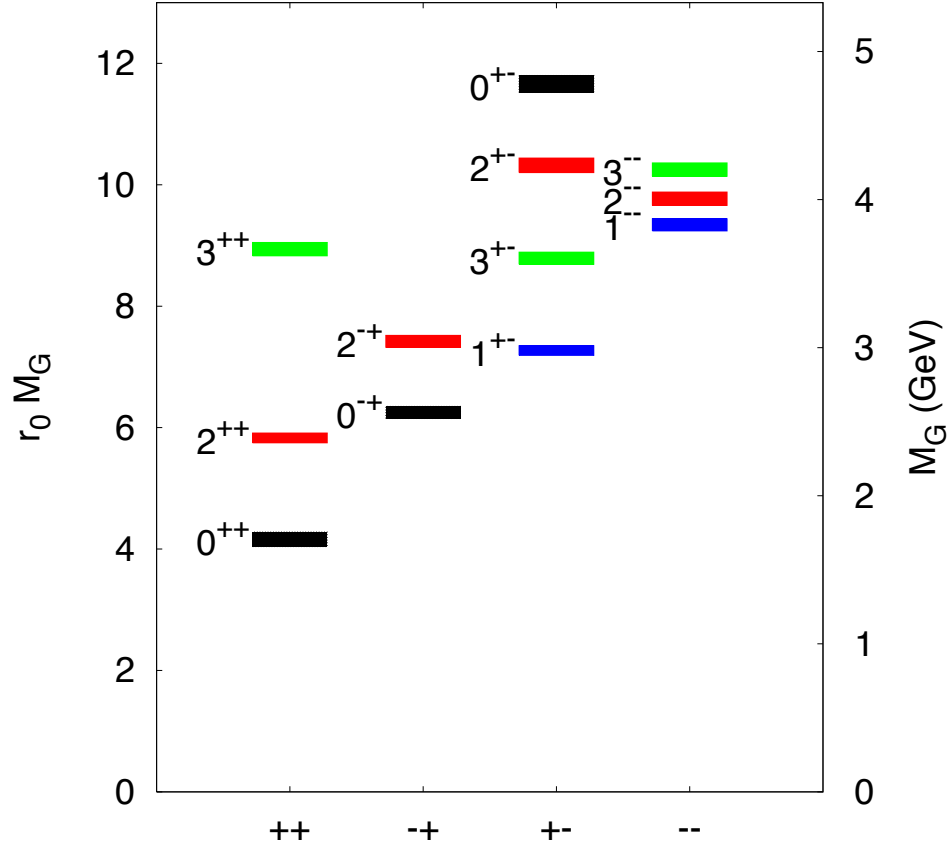


Figure 14.3: Predicted glueball mass spectrum from the lattice (from Ref. 9). See full-color version on color pages at end of book.

These lattice calculations assumed that the quark masses are infinite and neglect $q\bar{q}$ loops. However, one expects that glueballs will mix with nearby $q\bar{q}$ states of the same quantum numbers [7,14]. For example, the two isoscalar 0^{++} mesons will mix with the pure ground state glueball to generate the observed physical states $f_0(1370)$, $f_0(1500)$, and $f_0(1710)$. Experimental evidence is mounting that the $f_0(1500)$ has considerable affinity for glue, and that the $f_0(1370)$ and $f_0(1710)$ have large $u\bar{u} + d\bar{d}$ and $s\bar{s}$ components, respectively. The $f_0(1710)$ has also been proposed as a candidate scalar glueball [11] (see the “Note on Non- $q\bar{q}$ Mesons” at the end of the Meson Listings and Ref. 15).

Mesons made of $q\bar{q}$ pairs bound by excited gluons g , the hybrid states $q\bar{q}g$, are also predicted. They should lie in the 1.9 GeV mass region, according to gluon flux tube models [16]. Lattice QCD also predicts the lightest hybrid, an exotic 1^{-+} , at a mass of 1.9 GeV [17]. However, the bag model predicts four nonets, among them an exotic 1^{-+} around or above 1.4 GeV [18,19]. There are so far two candidates for exotic states with quantum numbers 1^{-+} , the $\pi_1(1400)$ and $\pi_1(1600)$, which could be hybrids or four-quark states (see the “Note on Non- $q\bar{q}$ Mesons” at the end of the Meson Listings and Ref. 15).

10 14. Quark model

14.4. Baryons: qqq states

Baryons are fermions with baryon number $\mathcal{B} = 1$, *i.e.*, in the most general case, they are composed of three quarks plus any number of quark - antiquark pairs. Although recently some experimental evidence for $(qqqq\bar{q})$ pentaquark states has been claimed (see review on Possible exotic baryon resonance), so far all established baryons are 3-quark (qqq) configurations. The color part of their state functions is an SU(3) singlet, a completely antisymmetric state of the three colors. Since the quarks are fermions, the state function must be antisymmetric under interchange of any two equal-mass quarks (up and down quarks in the limit of isospin symmetry). Thus it can be written as

$$|qqq\rangle_A = |\text{color}\rangle_A \times |\text{space, spin, flavor}\rangle_S, \quad (14.21)$$

where the subscripts S and A indicate symmetry or antisymmetry under interchange of any two equal-mass quarks. Note the contrast with the state function for the three nucleons in ${}^3\text{H}$ or ${}^3\text{He}$:

$$|NNN\rangle_A = |\text{space, spin, isospin}\rangle_A. \quad (14.22)$$

This difference has major implications for internal structure, magnetic moments, *etc.* (For a nice discussion, see Ref. 20.)

The “ordinary” baryons are made up of u , d , and s quarks. The three flavors imply an approximate flavor SU(3), which requires that baryons made of these quarks belong to the multiplets on the right side of

$$\mathbf{3} \otimes \mathbf{3} \otimes \mathbf{3} = \mathbf{10}_S \oplus \mathbf{8}_M \oplus \mathbf{8}_M \oplus \mathbf{1}_A \quad (14.23)$$

(see Sec. 37, on “SU(n) Multiplets and Young Diagrams”). Here the subscripts indicate symmetric, mixed-symmetry, or antisymmetric states under interchange of any two quarks. The $\mathbf{1}$ is a uds state (Λ_1), and the octet contains a similar state (Λ_8). If these have the same spin and parity, they can mix. The mechanism is the same as for the mesons (see above). In the ground state multiplet, the SU(3) flavor singlet Λ_1 is forbidden by Fermi statistics. Section 36, on “SU(3) Isoscalar Factors and Representation Matrices,” shows how relative decay rates in, say, $\mathbf{10} \rightarrow \mathbf{8} \otimes \mathbf{8}$ decays may be calculated.

The addition of the c quark to the light quarks extends the flavor symmetry to SU(4). However, due to the large mass of the c quark, this symmetry is much more strongly broken than the SU(3) of the three light quarks. Figures 14.4(a) and 14.4(b) show the SU(4) baryon multiplets that have as their bottom levels an SU(3) octet, such as the octet that includes the nucleon, or an SU(3) decuplet, such as the decuplet that includes the $\Delta(1232)$. All particles in a given SU(4) multiplet have the same spin and parity. The charmed baryons are discussed in more detail in the “Note on Charmed Baryons” in the Particle Listings. The addition of a b quark extends the flavor symmetry to SU(5), the existence of baryons with t -quarks is very unlikely due to the short lifetime of the top.

For the “ordinary” baryons (no c or b quark), flavor and spin may be combined in an approximate flavor-spin SU(6), in which the six basic states are $d \uparrow$, $d \downarrow$, \dots , $s \downarrow$ (\uparrow , \downarrow = spin up, down). Then the baryons belong to the multiplets on the right side of

$$\mathbf{6} \otimes \mathbf{6} \otimes \mathbf{6} = \mathbf{56}_S \oplus \mathbf{70}_M \oplus \mathbf{70}_M \oplus \mathbf{20}_A. \quad (14.24)$$

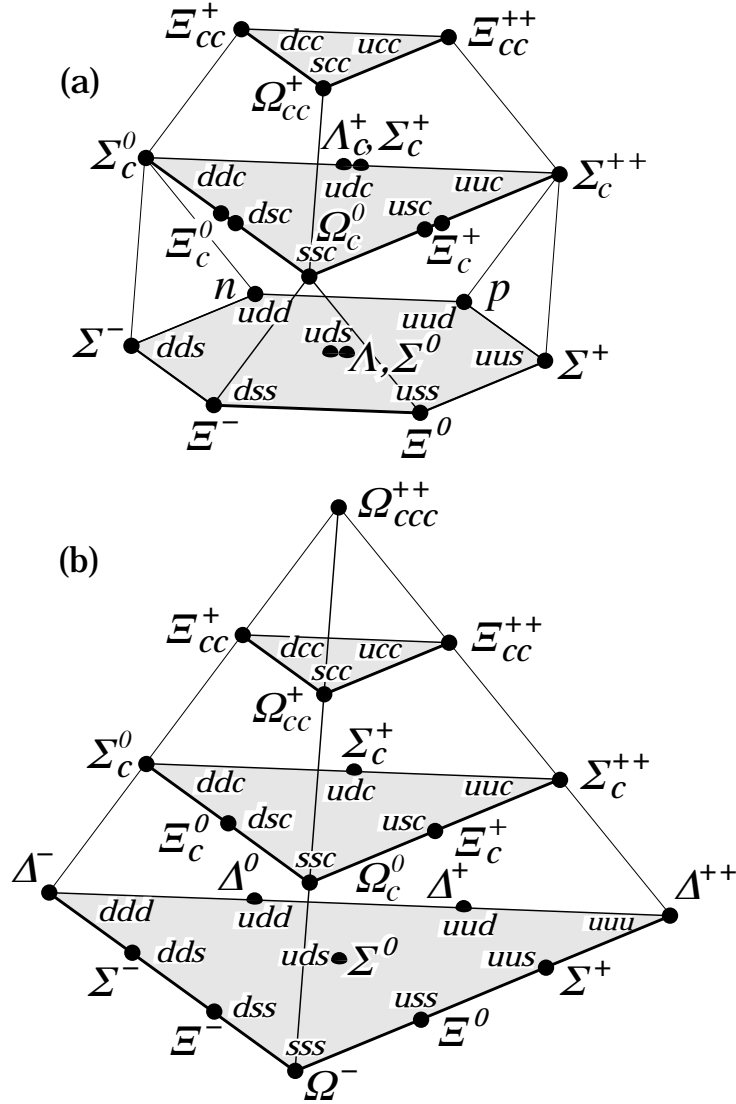


Figure 14.4: SU(4) multiplets of baryons made of u , d , s , and c quarks. (a) The 20-plet with an SU(3) octet. (b) The 20-plet with an SU(3) decuplet.

These SU(6) multiplets decompose into flavor SU(3) multiplets as follows:

$$56 = {}^4\mathbf{10} \oplus {}^2\mathbf{8} \quad (14.25a)$$

$$70 = {}^2\mathbf{10} \oplus {}^4\mathbf{8} \oplus {}^2\mathbf{8} \oplus {}^2\mathbf{1} \quad (14.25b)$$

$$20 = {}^2\mathbf{8} \oplus {}^4\mathbf{1}, \quad (14.25c)$$

where the superscript $(2S + 1)$ gives the net spin S of the quarks for each particle in the SU(3) multiplet. The $J^P = 1/2^+$ octet containing the nucleon and the $J^P = 3/2^+$ decuplet containing the $\Delta(1232)$ together make up the “ground-state” 56-plet, in which the orbital angular momenta between the quark pairs are zero (so that the spatial part of the state function is trivially symmetric). The **70** and **20** require some excitation of the spatial part of the state function in

12 14. Quark model

order to make the overall state function symmetric. States with nonzero orbital angular momenta are classified in $SU(6)\otimes O(3)$ supermultiplets.

It is useful to classify the baryons into bands that have the same number N of quanta of excitation. Each band consists of a number of supermultiplets, specified by (D, L_N^P) , where D is the dimensionality of the $SU(6)$ representation, L is the total quark orbital angular momentum, and P is the total parity. Supermultiplets contained in bands up to $N = 12$ are given in Ref. 22. The $N = 0$ band, which contains the nucleon and $\Delta(1232)$, consists only of the $(56, 0_0^+)$ supermultiplet. The $N = 1$ band consists only of the $(70, 1_1^-)$ multiplet and contains the negative-parity baryons with masses below about 1.9 GeV. The $N = 2$ band contains five supermultiplets: $(56, 0_2^+)$, $(70, 0_2^+)$, $(56, 2_2^+)$, $(70, 2_2^+)$, and $(20, 1_2^+)$.

Table 14.5: N and Δ states in the $N=0,1,2$ harmonic oscillator bands. L^P denotes angular momentum and parity, S the three-quark spin and 'sym'=A,S,M the symmetry of the spatial wave function.

N	sym	L^P	S	$N(I = 1/2)$	$\Delta(I = 3/2)$
2	A	1^+	$1/2$	$1/2^+$	$3/2^+$
2	M	2^+	$3/2$	$1/2^+$	$3/2^+$ $5/2^+$ $7/2^+$
2	M	2^+	$1/2$	$3/2^+$	$5/2^+$ $3/2^+$ $5/2^+$
2	M	0^+	$3/2$	$3/2^+$	
2	M	0^+	$1/2$	$1/2^+$	$1/2^+$
2	S	2^+	$3/2$		$1/2^+$ $3/2^+$ $5/2^+$ $7/2^+$
2	S	2^+	$1/2$	$3/2^+$	$5/2^+$
2	S	0^+	$3/2$		$3/2^+$
2	S	0^+	$1/2$	$1/2^+$	
1	M	1^-	$3/2$	$1/2^-$	$3/2^-$ $5/2^-$
1	M	1^-	$1/2$	$1/2^-$	$3/2^-$ $1/2^-$ $3/2^-$
0	S	0^+	$3/2$		$3/2^+$
0	S	0^+	$1/2$	$1/2^+$	

The wave functions of the non-strange baryons in the harmonic oscillator basis are often labeled by $|X^{2S+1}L_\pi J^P\rangle$, where S, L, J, P are as above, $X = N$ or Δ , and $\pi = S, M$ or A denotes the symmetry of the spatial wave function. The possible states for the bands with $N=0,1,2$ are given in Table 14.5.

In Table 14.6, quark-model assignments are given for many of the established baryons whose $SU(6)\otimes O(3)$ compositions are relatively unmixed. One must, however, keep in mind that apart from the mixing of the Λ singlet and octet states, states with same J^P but different L, S combinations can also mix. In the quark model with one-gluon exchange motivated interactions, the size of the mixing is determined by the relative strength of the tensor term with respect to the contact term (see below). The mixing is more important for the decay patterns of the states than for their positions. An example are the lowest lying $(70, 1_1^-)$ states with $J^P=1/2^-$ and $3/2^-$. The physical states are:

Table 14.6: Quark-model assignments for some of the known baryons in terms of a flavor-spin SU(6) basis. Only the dominant representation is listed. Assignments for several states, especially for the $\Lambda(1810)$, $\Lambda(2350)$, $\Xi(1820)$, and $\Xi(2030)$, are merely educated guesses. For assignments of the charmed baryons, see the “Note on Charmed Baryons” in the Particle Listings.

J^P	(D, L_N^P)	S	Octet members			Singlets
$1/2^+$	$(56, 0_0^+)$	$1/2$	$N(939)$	$\Lambda(1116)$	$\Sigma(1193)$	$\Xi(1318)$
$1/2^+$	$(56, 0_2^+)$	$1/2$	$N(1440)$	$\Lambda(1600)$	$\Sigma(1660)$	$\Xi(?)$
$1/2^-$	$(70, 1_1^-)$	$1/2$	$N(1535)$	$\Lambda(1670)$	$\Sigma(1620)$	$\Xi(?)$ $\Lambda(1405)$
$3/2^-$	$(70, 1_1^-)$	$1/2$	$N(1520)$	$\Lambda(1690)$	$\Sigma(1670)$	$\Xi(1820)$ $\Lambda(1520)$
$1/2^-$	$(70, 1_1^-)$	$3/2$	$N(1650)$	$\Lambda(1800)$	$\Sigma(1750)$	$\Xi(?)$
$3/2^-$	$(70, 1_1^-)$	$3/2$	$N(1700)$	$\Lambda(?)$	$\Sigma(?)$	$\Xi(?)$
$5/2^-$	$(70, 1_1^-)$	$3/2$	$N(1675)$	$\Lambda(1830)$	$\Sigma(1775)$	$\Xi(?)$
$1/2^+$	$(70, 0_2^+)$	$1/2$	$N(1710)$	$\Lambda(1810)$	$\Sigma(1880)$	$\Xi(?)$ $\Lambda(?)$
$3/2^+$	$(56, 2_2^+)$	$1/2$	$N(1720)$	$\Lambda(1890)$	$\Sigma(?)$	$\Xi(?)$
$5/2^+$	$(56, 2_2^+)$	$1/2$	$N(1680)$	$\Lambda(1820)$	$\Sigma(1915)$	$\Xi(2030)$
$7/2^-$	$(70, 3_3^-)$	$1/2$	$N(2190)$	$\Lambda(?)$	$\Sigma(?)$	$\Xi(?)$ $\Lambda(2100)$
$9/2^-$	$(70, 3_3^-)$	$3/2$	$N(2250)$	$\Lambda(?)$	$\Sigma(?)$	$\Xi(?)$
$9/2^+$	$(56, 4_4^+)$	$1/2$	$N(2220)$	$\Lambda(2350)$	$\Sigma(?)$	$\Xi(?)$
Decuplet members						
$3/2^+$	$(56, 0_0^+)$	$3/2$	$\Delta(1232)$	$\Sigma(1385)$	$\Xi(1530)$	$\Omega(1672)$
$3/2^+$	$(56, 0_2^+)$	$3/2$	$\Delta(1600)$	$\Sigma(?)$	$\Xi(?)$	$\Omega(?)$
$1/2^-$	$(70, 1_1^-)$	$1/2$	$\Delta(1620)$	$\Sigma(?)$	$\Xi(?)$	$\Omega(?)$
$3/2^-$	$(70, 1_1^-)$	$1/2$	$\Delta(1700)$	$\Sigma(?)$	$\Xi(?)$	$\Omega(?)$
$5/2^+$	$(56, 2_2^+)$	$3/2$	$\Delta(1905)$	$\Sigma(?)$	$\Xi(?)$	$\Omega(?)$
$7/2^+$	$(56, 2_2^+)$	$3/2$	$\Delta(1950)$	$\Sigma(2030)$	$\Xi(?)$	$\Omega(?)$
$11/2^+$	$(56, 4_4^+)$	$3/2$	$\Delta(2420)$	$\Sigma(?)$	$\Xi(?)$	$\Omega(?)$

$$|S_{11}(1535)\rangle = \cos(\theta_S)|N^2P_M1/2^-\rangle - \sin(\theta_S)|N^4P_M1/2^-\rangle \quad (14.26)$$

$$|D_{13}(1520)\rangle = \cos(\theta_D)|N^2P_M3/2^-\rangle - \sin(\theta_D)|N^4P_M3/2^-\rangle \quad (14.27)$$

and the orthogonal combinations for $S_{11}(1650)$ and $D_{13}(1700)$. The mixing is large for the $J^P=1/2^-$ states ($\theta_S \approx -32^\circ$), but small for the $J^P=3/2^-$ states ($\theta_D \approx +6^\circ$) [23], [26].

All baryons of the ground state multiplets are known. Many of their properties (masses, magnetic moments *etc.*) are in good agreement with the most basic versions of the quark model, including harmonic (or linear) confinement and a spin-spin interaction, which is responsible for the octet - decuplet mass shifts.

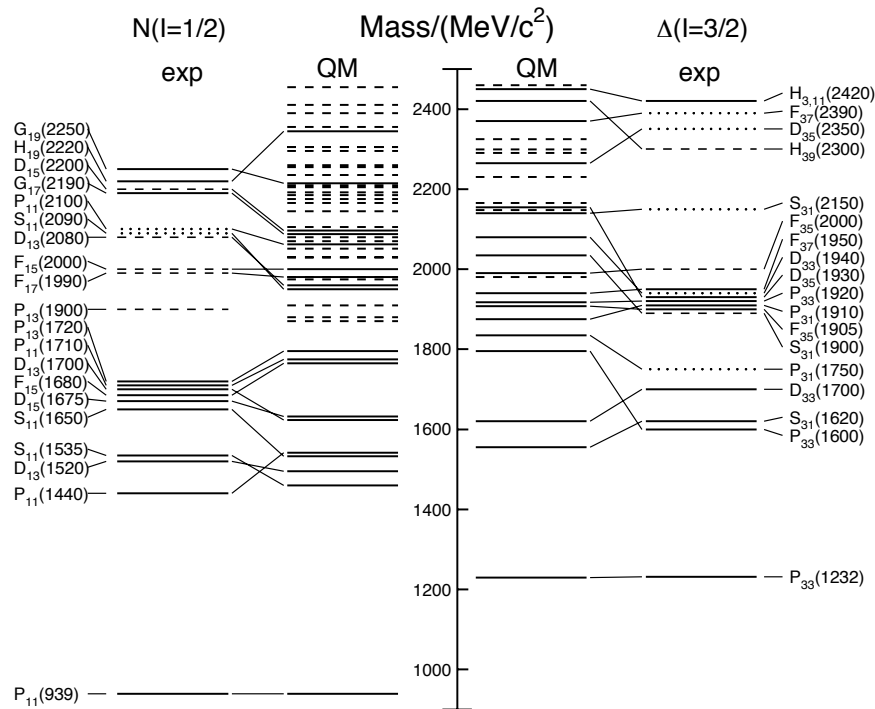


Figure 14.5: Excitation spectrum of the nucleon. Compared are the positions of the excited states identified in experiment, to those predicted by a modern quark model calculation. Left hand side: isospin $I = 1/2$ N -states, right hand side: isospin $I = 3/2$ Δ -states. Experimental: (columns labeled 'exp'), three and four star states are indicated by full lines (two-star dashed lines, one-star dotted lines). At the very left and right of the figure, the spectroscopic notation of these states is given. Quark model [24]: (columns labeled 'QM'), all states for the $N=1,2$ bands, low-lying states for the $N=3,4,5$ bands. Full lines: at least tentative assignment to observed states, dashed lines: so far no observed counterparts. Many of the assignments between predicted and observed states are highly tentative.

The situation for the excited states is much less clear. There are two main problems which are illustrated in Fig. 14.5, where the experimentally observed excitation spectrum of the nucleon (N and Δ resonances) is compared to the results of a typical quark model calculation [24]. Many more states are predicted than observed, but on the other hand, states with certain quantum numbers appear in the spectrum at excitation energies much lower than predicted. Up to an excitation energy of 2.4 GeV, about 45 N states are predicted, but only 12 are established (four or three star; see Note on N and Δ Resonances for the rating of the status of resonances) and 7 are tentative (two or one star). Even for the $N=1,2$ bands, up to now only half of the predicted states have been observed. This has been known for a long time as the 'missing resonance' problem [23]. On the other hand, the lowest states from the $N=2$ band, the $P_{11}(1440)$ and the $P_{33}(1600)$, appear lower than the negative parity states from the $N=1$ band, and much lower than predicted by most models. Also negative parity Δ states from the $N=3$ band ($S_{31}(1900)$, $D_{33}(1940)$, and $D_{35}(1930)$) are too low in energy. Part of the problem could be experimental. Among the negative parity Δ states, only the D_{35} has three stars and the uncertainty in the position of the $P_{33}(1600)$ is large (1550 - 1700 MeV). For the missing resonance problem, selection rules could play a role [23]. The states are broad and overlapping, and most studies of baryon resonances have been done with pion-induced reactions, so that there is bias in the data base against resonances,

which couple only weakly to the $N\pi$ channel. Quark model predictions for the couplings to other hadronic channels and to photons are given in Ref. 24. A large experimental effort is ongoing at several electron accelerators to study the baryon resonance spectrum with real and virtual photon-induced meson production reactions. This includes the search for as-yet-unobserved states, as well as detailed studies of the properties of the low lying states (decay patterns, electromagnetic couplings, magnetic moments, *etc.*) (see Ref. 25 for recent reviews).

In quark models, the number of excited states is determined by the effective degrees of freedom, while their ordering and decay properties are related to the residual quark - quark interaction. A recent overview of quark models for baryons is given in Ref. 26. The effective degrees of freedom in the standard nonrelativistic quark model are three equivalent valence quarks with one-gluon exchange-motivated, flavor-independent color magnetic interactions. A different class of models uses interactions which give rise to a quark - diquark clustering of the baryons (for a review see Ref. 27). If there is a tightly bound diquark, only two degrees of freedom are available at low energies, and thus *fewer* states are predicted. Furthermore, selection rules in the decay pattern may arise from the quantum numbers of the diquark. *More* states are predicted by collective models of the baryon like the algebraic approach in Ref. 28. In this approach, the quantum numbers of the valence quarks are distributed over a Y-shaped string-like configuration, and additional states arise *e.g.*, from vibrations of the strings. *More* states are also predicted in the framework of flux-tube models (see [29]), which are motivated by lattice QCD. In addition to the quark degrees of freedom, flux-tubes responsible for the confinement of the quarks are considered as degrees of freedom. These models include hybrid baryons containing explicit excitations of the gluon fields. However, since all half integral J^P quantum numbers are possible for ordinary baryons, such ‘exotics’ will be very hard to identify, and probably always mix with ordinary states. So far, the experimentally observed number of states is still far lower even than predicted by the quark-diquark models.

14.5. Dynamics

Many specific quark models exist, but most contain a similar basic set of dynamical ingredients. These include:

- i) A confining interaction, which is generally spin-independent (*e.g.*, harmonic oscillator or linear confinement).
- ii) Different types of spin-dependent interactions:
 - a) commonly used is a color magnetic flavor-independent interaction modeled after the effects of gluon exchange in QCD (see *e.g.*, Ref. 31). For example, in the S -wave states, there is a spin-spin hyperfine interaction of the form

$$H_{HF} = -\alpha_S M \sum_{i>j} (\vec{\sigma} \lambda_a)_i (\vec{\sigma} \lambda_a)_j , \quad (14.28)$$

where M is a constant with units of energy, λ_a ($a = 1, \dots, 8$) is the set of SU(3) unitary spin matrices, defined in Sec. 36, on “SU(3) Isoscalar Factors and Representation Matrices,” and the sum runs over constituent quarks or antiquarks. Spin-orbit interactions, although allowed, seem to be small in general, but a tensor term is responsible for the mixing of states with the same J^P but different L, S combinations.

b) other approaches include flavor-dependent short-range quark forces from instanton effects (see *e.g.*, Ref. 32). This interaction acts only on scalar, isoscalar pairs of quarks in a relative s-wave state:

$$\langle q^2; S, L, T | W | q^2; S, L, T \rangle = -4g\delta_{S,0}\delta_{L,0}\delta_{I,0}\mathcal{W} \quad (14.29)$$

16 14. Quark model

where \mathcal{W} is the radial matrix element of the contact interaction.

c) a rather different and controversially discussed approach is based on flavor-dependent spin-spin forces arising from one-boson exchange. The interaction term is of the form:

$$H_{HF} \propto \sum_{i < j} V(\vec{r}_{ij}) \lambda_i^F \cdot \lambda_j^F \vec{\sigma}_i \cdot \vec{\sigma}_j \quad (14.30)$$

where the λ_i^F are in flavor space (see *e.g.*, Ref. 33).

- iii) A strange quark mass somewhat larger than the up and down quark masses, in order to split the SU(3) multiplets.
- iv) In the case of spin-spin interactions (ii,a,c), a flavor symmetric interaction for mixing $q\bar{q}$ configurations of different flavors (*e.g.*, $u\bar{u} \leftrightarrow d\bar{d} \leftrightarrow s\bar{s}$), in isoscalar channels, so as to reproduce *e.g.*, the η - η' and ω - Φ mesons.

These ingredients provide the basic mechanisms that determine the hadron spectrum in the standard quark model.*

14.6. Lattice Calculations of Hadronic Spectroscopy

Lattice calculations predict the spectrum of bound states in QCD from first principles, beginning with the Lagrangian of full QCD or of various approximations to it. This is typically done using the Euclidean path integral formulation of quantum field theory, where the analog of a partition function for a field theory containing some generic fields $\phi(x)$, with action $S(\phi)$, is

$$Z = \int [d\phi] \exp(-S(\phi)). \quad (14.31)$$

The expectation value of any observable O is

$$\langle O \rangle = \frac{1}{Z} \int [d\phi] O(\phi) \exp(-S(\phi)). \quad (14.32)$$

The theory is regulated by introducing a space-time lattice, with lattice spacing a . This converts the functional integral Eq. (14.31) into an ordinary integral (of very large dimensionality). The integral is replaced by a Monte Carlo sampling over an ensemble of configurations of field variables, using an algorithm which insures that a field configuration is present in the ensemble with a probability proportional to $\exp(-S(\phi_j))$. Then ensemble averages become sample averages,

$$\langle O \rangle = \frac{1}{N} \sum_{j=1}^N O(\phi_j). \quad (14.33)$$

This is all quite similar to the kind of Monte Carlo simulation done by experiments, except that the ensembles of field configurations are created sequentially, as a so-called ‘‘Markov chain.’’

In QCD, the field variables correspond to gauge fields and quark fields. In a lattice calculation, the lattice spacing (which serves as an ultraviolet cutoff) and the (current) quark masses are inputs; hadron masses and other observables are predicted as a function of those masses. The

* However, recently, in a radically different approach [30], it has been suggested that most baryon and meson resonances can be generated by chiral coupled channel dynamics.

lattice spacing is unphysical, and it is necessary to extrapolate to the limit of zero lattice spacing. Lattice predictions are for dimensionless ratios of dimensionful parameters (like mass ratios) and predictions of dimensionful quantities require using one experimental input to set the scale. Interpolation or extrapolation of lattice results in the light quark masses involves formulas of chiral perturbation theory.

For conventional hadronic states, lattice calculations use the quark model to construct operators, which are taken as interpolating fields. This does not mean that the hadronic states have minimal quark content: the operators create multi-quark states with particular quantum numbers, but they are connected by quark propagators which include all effects of relativity, and could include the effects of virtual quark-antiquark pairs in the vacuum.

Constituent gluons do not appear naturally in lattice calculations; instead, gauge fields appear as link variables, which allow color to be parallel transported across the lattice in a gauge covariant way. Calculations of glueballs on the lattice use interpolating fields of the form $O_j \sim \exp i \oint \vec{A} \cdot \vec{d}l$ integrated about some path. The fields look like closed tubes of chromoelectric and chromomagnetic flux. Calculations of exotics are done with interpolating fields involving quark and antiquark creation operators joined by flux tubes.

Calculations with heavy quarks typically use Non-Relativistic QCD (NRQCD) or Heavy Quark Effective Theory (HQET), systematic expansions of the QCD Lagrangian in powers of the heavy quark velocity or the inverse heavy quark mass. Terms in the Lagrangian have obvious quark model analogs, but are derived directly from QCD. The heavy quark potential is a derived quantity, measured in simulations.

Lattice calculations are as specialized as the experiments which produce the data in this book, and it is not easy to give a blanket answer to the question: “how well can lattice calculations predict” any specific quantity? However, let us try:

The cleanest lattice predictions come from measurements of processes in which there is only one particle in the simulation volume. These quantities include masses of hadrons, simple decay constants, like pseudoscalar meson decay constants, and semileptonic form factors (such as the ones appropriate to $B \rightarrow D l \nu$, $K l \nu$, $\pi l \nu$). The cleanest predictions for masses are for states which have narrow decay widths and are far below any thresholds to open channels, since the effects of final state interactions are not yet under complete control on the lattice. “Difficult” states for the quark model (such as exotics) are also difficult for the lattice because of the lack of simple operators which couple well to them. Technical issues presently prevent lattice practitioners from directly computing matrix elements for weak decays with more than one strongly interacting particle in the final state.

Good-quality modern lattice calculations will present multi-part error budgets with their predictions. Users are advised to read them carefully! A small part of the uncertainty is statistical, from sample size. Typically, the quoted statistical uncertainty includes uncertainty from a fit: it is rare that a simulation measures one global quantity which is the desired observable. Simulations with light dynamical quarks are typically done at mass values heavier than the experimental ones, and it is necessary to extrapolate in the quark mass. They are always done at nonzero lattice spacing, and so it will be necessary to extrapolate to zero lattice spacing. Some theoretical input is needed to do this. Much of the uncertainty in these extrapolations is systematic, from the choice of fitting function. Other systematics include the number of dynamical flavors of quarks actually simulated, and technical issues with how these dynamical quarks are included. The particular choice of a fiducial mass (to normalize other predictions) is not standardized; there are many possible choices, each with its own set of strengths and weaknesses, and determining it usually requires a second lattice simulation from that used to calculate the quantity under consideration.

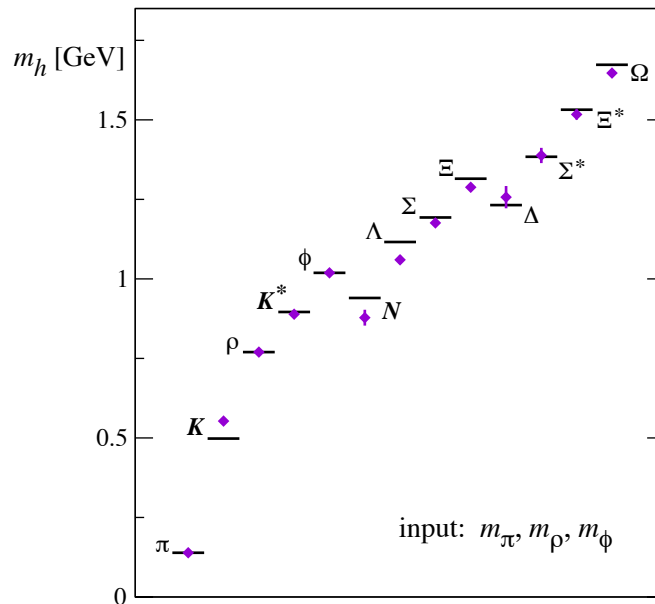


Figure 14.6: Comparison of quenched results with experiment, from Ref. 34 as presented by Ref. 35.

Of course, there is much more to lattice calculations besides spectroscopy; please refer to the mini-review on Quark Masses in the Quarks section of the Listings for more lattice-based phenomenology.

We conclude with a few “representative” pictures of spectroscopy from recent state-of-the-art simulations. They illustrate (better than any discussion) the size of lattice uncertainties.

A systematic of major historical interest is the “quenched approximation,” in which virtual quark-antiquark pairs are simply left out of the simulation. This was done because the addition of these virtual pairs presented an expensive computational problem. Recent advances in algorithms and computer hardware have rendered it obsolete. A recent quenched simulation [34] of the light hadron spectrum is shown in Fig. 14.6. Note the qualitative quark model features of the lattice result: the equal spacing of the decuplet and the vector meson multiplet. The lattice error bars are small enough to reveal systematic errors in the quenched approximation: note especially, that the kaon and ϕ masses cannot be simultaneously correctly determined, and the nucleon/rho meson mass ratio is too low. No generally-accepted methodology has ever allowed one to correct for quenching effects, short of redoing all calculations with dynamical quarks.

Fig. 14.7 from Ref. 36 shows a comparison of quenched spectroscopy with results from a simulation with a strange quark at roughly its physical value, and two flavors of light dynamical quarks with masses at roughly one fifth of the strange quark’s mass. The authors focus on quantities for which lattice predictions should work well, as we described above. The left panel shows these authors’ compilation of quenched results; the right panel, results with dynamical fermions, after a chiral extrapolation.

Fig. 14.8 shows Upsilon ($b\bar{b}$) spectroscopy from Ref. 37. The calculation uses a discretization of nonrelativistic QCD for its heavy quarks, and includes three flavors of light dynamical staggered fermions. Quenched data are also shown for comparison.

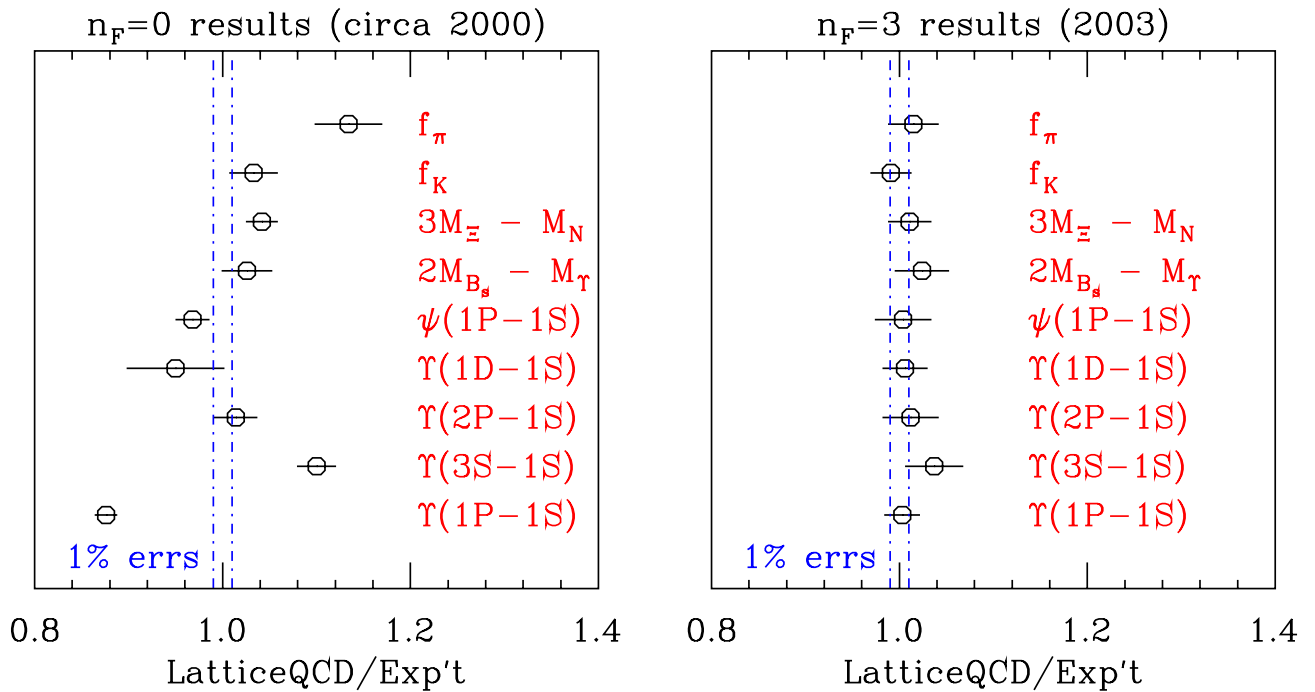


Figure 14.7: Comparison of quenched results with results from simulations with 2+1 flavors of staggered fermions, from Ref. [36].

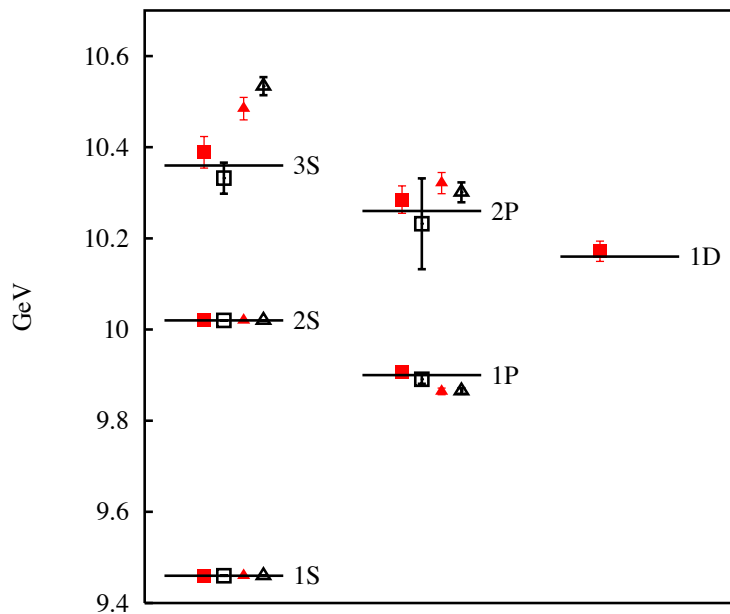


Figure 14.8: The T spectrum of radial and orbital levels from Ref. [37]. Closed and open symbols are from coarse and fine lattices respectively. Squares and triangles denote unquenched and quenched results respectively. Lines represent experiment. See full-color version on color pages at end of book.

References:

1. J. Schwinger, Phys. Rev. Lett. **12**, 237 (1964).
2. A. Bramon *et al.*, Phys. Lett. **B403**, 339 (1997).
3. A. Aloisio *et al.*, Phys. Lett. **B541**, 45 (2002).
4. C. Amsler *et al.*, Phys. Lett. **B294**, 451 (1992).
5. C. Amsler, Rev. Mod. Phys. **70**, 1293 (1998).
6. T. Feldmann, Int. J. Mod. Phys. **A915**, 159 (2000).
7. C. Amsler and F.E. Close, Phys. Rev. **D53**, 295 (1996).
8. R.L. Jaffe, Phys. Rev. **D 15** 267, 281 (1977).
9. Y. Chen *et al.*, Phys. Rev. **D73**, 014516 (2006).
10. C. Morningstar and M. Peardon, Phys. Rev. **D60**, 034509 (1999).
11. W. J. Lee and D. Weingarten, Phys. Rev. **D61**, 014015 (2000).
12. G. S. Bali, *et. al.* Phys. Lett. **B309**, 378 (1993).
13. C. Michael, AIP Conf. Proc. **432**, 657 (1998).
14. F.E. Close and A. Kirk, Eur. Phys. J. **C21**, 531 (2001).
15. C. Amsler and N.A. Törnqvist, Phys. Rev. **389**, 61 (2004).
16. N. Isgur and J. Paton, Phys. Rev. **D31**, 2910 (1985).
17. P. Lacock *et al.*, Phys. Lett. **B401**, 308 (1997);
C. Bernard *et al.*, Phys. Rev. **D56**, 7039 (1997).
18. M. Chanowitz and S. Sharpe, Nucl. Phys. **B222**, 211 (1983).
19. T. Barnes *et al.*, Nucl. Phys. **B224**, 241 (1983).
20. F.E. Close, in *Quarks and Nuclear Forces* (Springer-Verlag, 1982), p. 56.
21. Particle Data Group, Phys. Lett. **111B** (1982).
22. R.H. Dalitz and L.J. Reinders, in *Hadron Structure as Known from Electromagnetic and Strong Interactions, Proceedings of the Hadron '77 Conference* (Veda, 1979), p. 11.
23. N. Isgur and G. Karl, Phys. Rev. **D18**, 4187 (1978); *ibid.*, **D19**, 2653 (1979); *ibid.*, **D20**, 1191 (1979);
K.-T. Chao *et al.*, Phys. Rev. **D23**, 155 (1981).
24. S. Capstick and W. Roberts, Phys. Rev. **D49**, 4570 (1994); *ibid.*, **D57**, 4301 (1998); *ibid.*, **D58**, 074011 (1998);
S. Capstick, Phys. Rev. **D46**, 2864 (1992).
25. B. Krusche and S. Schadmand, Prog. Part. Nucl. Phys. **51**, 399 (2003);
V.D. Burkert and T.-S.H. Lee, Int. J. Mod. Phys. **E13**, 1035 (2004).
26. S. Capstick and W. Roberts, Prog. Part. Nucl. Phys. **45**, 241 (2000);
see also A.J.G. Hey and R.L. Kelly, Phys. Reports **96**, 71 (1983).
27. M. Anselmino *et al.*, Rev. Mod. Phys. **65**, 1199 (1993).
28. R. Bijker *et al.*, Ann. of Phys. **236** 69 (1994).
29. N. Isgur and J. Paton, Phys. Rev. **D31**, 2910 (1985);
S. Capstick and P.R. Page, Phys. Rev. **C66**, 065204 (2002).
30. M.F.M Lutz and E.E. Kolomeitsev, Nucl. Phys. **A700**, 193 (2002);
M.F.M Lutz and E.E. Kolomeitsev, Nucl. Phys. **A730**, 392 (2004);
E.E. Kolomeitsev and M.F.M Lutz, Phys. Lett. **B585**, 243 (2004).
31. A. De Rujula *et al.*, Phys. Rev. **D12**, 147 (1975).
32. W.H. Blask *et al.*, Z. Phys. **A337** 327 (1990);
U. Löring *et al.*, Eur. Phys. J. **A10** 309 (2001);
U. Löring *et al.*, Eur. Phys. J. **A10** 395 (2001); *ibid.*, **A10** 447 (2001).
33. L.Y. Glozman and D.O. Riska, Phys. Rept. **268** 263 (1996);
L.Y. Glozman *et al.*, Phys. Rev. **D58**, 094030 (1998).

34. S. Aoki *et al.* [CP-PACS Collaboration], Phys. Rev. D **67**, 034503 (2003) [arXiv:hep-lat/0206009].
35. M. Luscher, Annales Henri Poincare **4**, S197 (2003) [arXiv:hep-ph/0211220].
36. C. T. H. Davies *et al.* [HPQCD Collaboration], Phys. Rev. Lett. **92**, 022001 (2004) [arXiv:hep-lat/0304004].
37. A. Gray *et al.*, Phys. Rev. D **72**, 094507 (2005) [arXiv:hep-lat/0507013].